

SCIENTIFIC REPORTS



OPEN

A comparison of hydrological and topological watersheds

B. Burger¹, J. S. Andrade Jr.^{1,2} & H. J. Herrmann^{1,2}

We introduce the hydrological watershed, a watershed where water can penetrate the soil, and compare it with the topological watershed for a two-dimensional landscape. For this purpose, we measure the fractal dimension of the hydrological watershed for different penetration depths and different grid sizes. Through finite size scaling, we find that the fractal dimension is 1.31 ± 0.02 which is significantly higher than the fractal dimension of the topological watershed. This indicates that the hydrological watershed belongs to a new universality class. We also find that, as opposed to the topological watershed, the hydrodynamic watershed can exhibit disconnected islands.

Watersheds separate hydrological basins and are an intrinsic property of landscapes^{1–4}. Rooted in geomorphology, watersheds play an important role in water management^{5,6} and are as such connected to topological studies about the water retention capacity⁷. They can also be encountered when defining the borders of countries, as seen in the case of Chile and Argentina⁸ or Switzerland and Italy⁹. While watersheds are directly related to percolation theory^{10,11}, they furthermore have applications in medicine^{12,13} and image processing^{14,15}.

An interesting property of watersheds is their self-similar character¹⁶. Fractality is a general, important property of physical structures and in the case of watersheds it can be used to deduce the length of the watershed in dependency of the scale. This can be helpful to correctly estimate the length of watersheds when rescaling digital maps. The fractal dimension of an object is also a measure for its structure, as two objects with different fractal dimensions will scale differently. It can furthermore connect phenomena that are at first glance seemingly unconnected physical problems if they have the same universal fractal dimension^{17–20}. For artificial landscapes and for digital elevation models, the fractal dimensions of watersheds have already been calculated under the condition that water only flows on the surface and can not penetrate into the soil, which we will call here the *topological watershed*^{21–25}. This watershed is in the same universality class as the optimum path crack²⁶, the shortest path on loop-less percolation, polymers in strongly disordered media²⁷ and bridge percolation¹⁷. The topological watershed has been shown numerically to be SLE²⁸.

The question we address is how the structure of a topological watershed of a two-dimensional surface changes compared to a hydrological watershed, where water can penetrate the soil. Whether and how the fractal dimension of the watershed changes has not yet been investigated and is the subject of the present paper. To answer this question, we use a generalized version of the invasion percolation (IP) based²⁹ algorithm proposed by Fehr *et al.* in ref.²². Throughout this paper we use an uncorrelated, artificially generated landscape to investigate the structural changes in a more controllable environment.

Methods

For the definition of the hydrological watershed's landscape, we choose a three-dimensional grid consisting of sites i with heights h_i on the upper surface and permeabilities p_i below the surface. The heights h_i are chosen randomly between zero and one. In this way, we model different permeabilities of the soil which lead to different penetration depths. For a soil discretized as a cubic lattice with edge length L , we implement the penetration-hindrance such that the resistance increases systematically with increasing depth n_i . To control the seeping depth of the water, we generate the permeabilities p_i as the sum of a randomly generated part with an offset which depends on the layer n_i of site i given by,

$$p_i = r + an_i, \quad (1)$$

where r is a random number homogeneously distributed between 0 and 1, a is the parameter of the model which controls the depth the water reaches, and n_i is the layer of site i divided by the edge length L which also yields a number between 0 and 1.

¹IfB, HIT G23.1, ETH Zürich, Zürich, 8093, Switzerland. ²Departamento de Física, Universidade Federal do Ceará, Fortaleza, 60451-970, Ceará, Brazil. Correspondence and requests for materials should be addressed to B.B. (email: bastian.burger@bluewin.ch)

Received: 6 November 2017
Accepted: 15 June 2018
Published online: 12 July 2018

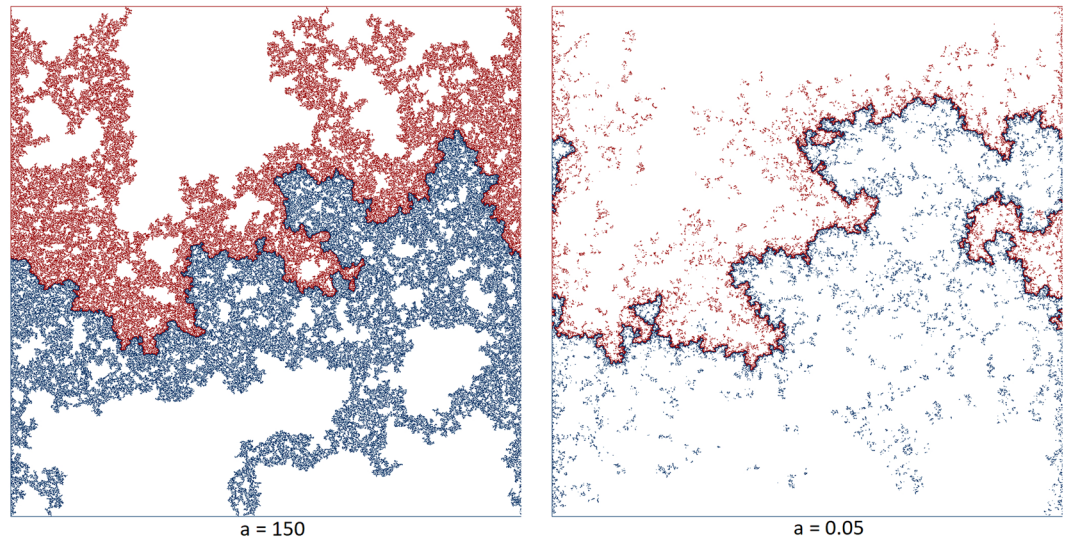


Figure 1. The dark line is the watershed extracted with the IP-based algorithm for three-dimensional models generated according to Eq. (1) for different a and grid length $L = 1000$. The red points belong to an IP-cluster that drains to the upper basin and the blue ones belong to an IP-cluster that drains to the lower basin. The figure was created by storing the top layer of the system as a bitmap.

The *outlets* of a terrain can be something like a river, underground river, a lake, or any other structure in which water can leave the system. We choose the outlets to be two opposite, vertical sides of the cube. Helical boundary conditions are implemented on the two non-outlet, vertical sides of the cube in order to make sure to keep the water inside the system, if it is not leaving at one of the two outlets. The helical boundary conditions on the non-outlet surfaces are implemented such that the neighbors of site i of a three-dimensional lattice stored in an array are given by the sites $i - 1, i + 1, i - L, i + L, i - L^2, i + L^2$. We do not have to care about the bottom boundary if we choose the depth of the cube to be greater than $d_{min} = \frac{1}{a}$. The water will never reach a layer larger than d_{min} because the permeability $p_{d_{min}}$ represents the maximum possible permeability of the upper surface $h_{max} = 1$ and, therefore, acts as a boundary for the seeping water.

The most important aspect for extracting the watershed is to find out to which outlet the water at site s drains to, thus to find in which *catchment basin* s lies. For this we follow a procedure that is called *growing an IP cluster*²², where IP stands for invasion percolation²⁹. p is the permeability for sites that are below the surface as well as the height of sites that are on the surface. Starting at s , the water takes the path of steepest descent. We denote the i^{th} site in the IP cluster with c_i . At each step $i > 1$, we add the neighbor of site c_{i-1} with the smallest $p_{c_{i-1}}$ to the cluster, but only if the $p_{neighbor}$ is smaller than $p_{c_{i-1}}$ and if it is not already belonging to the cluster. If for all neighbors $p_{neighbor}$ is larger than $p_{c_{i-1}}$, the cluster is stuck in a local minimum that we call a *pore*: A pore consists of all sites p that have the same p as c_{i-1} and is the equivalent of a lake in the case of a topological watershed. We flood the pore and add the neighbor n_{min} with the lowest permeability on its perimeter to the cluster, thus we set $c_i = n_{min}$. By repeating this procedure we will at the end always reach an outlet. We know that all sites of the same IP cluster drain to the same outlet and we thus label all sites c_i within one IP cluster as belonging to the same catchment basin. However, the procedure of growing IP clusters alone is not yet efficient if we grow them from each site of the surface. It is more convenient to start with one segment of the watershed. We label each adjacent site with the outlet to which the water flows by growing an IP cluster. The next segment of the watershed then comes to lie between the two adjacent sites that drain to different outlets of the system. By repeating this procedure we grow the watershed until it spans the system from one side to the other. The initial segment of the watershed can be found by moving from one outlet of the system to the other while growing IP clusters.

Data availability. The datasets generated during and/or analyzed during the current study are available from the corresponding author on reasonable request.

Results

The comparison between the landscape of a hydrological and a topological watershed shows that on the top layer of the hydrological case, less sites belong to an IP-cluster than for the topological case (see Fig. 1). This is a direct result of the penetration resistance. For $a \ll 1$, a large part of the IP-cluster's mass exists underground, whereas for $a \gg 1$, the water mostly stays at the surface, since its room for evasion into the soil is very small.

We find that as opposed to the topological watershed, the hydrological watershed is not always a connected line anymore, as islands can occur (see Fig. 2). An island is a region of connected sites belonging to a catchment basin i that is surrounded by sites belonging to catchment basin $j \neq i$. In Fig. 2 we can even observe the formation of islands within an island. We surmise that the size of these islands and their relative placement to the watershed depends on the penetration depth of the water, or, expressed equivalently, on the extent of three-dimensionality

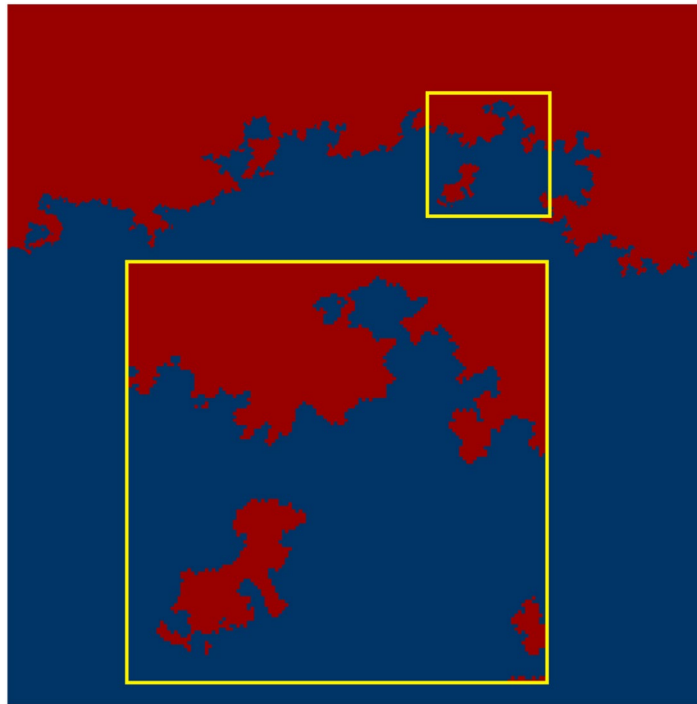


Figure 2. The top layer of a typical realization of a hydrological watershed, calculated for $a = 0.05$ and a grid length of $L = 1100$. Colors as in Fig. 1. The figure was created by storing the top layer of the system as a bitmap.

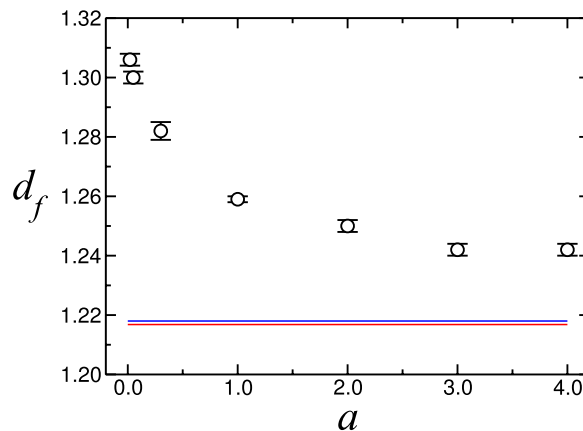


Figure 3. Measured fractal dimensions as a function of the depth parameter a . The blue line represents the value for $a = 1200$, while the red line represents the topological watershed corresponding to the asymptotic value $a \rightarrow \infty$, as reported by Fehr *et al.* in²².

of the landscape. The size of the islands as well as the distance from the watershed increases with decreasing penetration resistance.

Using the yardstick method³⁰ we measured the fractal dimension of the watershed for each simulated system, where the heights h_i and the permeabilities p_i are generated with a congruential number generator³¹. For each system i , we get a data set consisting of tuples containing the stick length ε and the number of sticks $N(\varepsilon)$ needed to approximate the watershed. The function $N(\varepsilon)$ satisfies $N(\varepsilon) \propto \varepsilon^{-d_{f,i}}$, where $d_{f,i}$ is the fractal dimension of the watershed of system i . For each value of a , we average the fractal dimension over N landscapes.

The results obtained for the fractal dimension show that for the hydrological watershed, the fractal dimension decreases with the model parameter a (see Fig. 3). From these data we linearly extrapolated the fractal dimension of the three smallest measurement values to the limit $a \rightarrow 0$ and found it to be 1.31 ± 0.02 . We obtained the error bar by finding the lines of maximum and minimum slope that still fit the data. For $a \rightarrow \infty$ the fractal dimension of the topological watershed is consistent with the high precision calculation by Fehr *et al.*, namely, 1.2168 ± 0.0005 ²⁴.

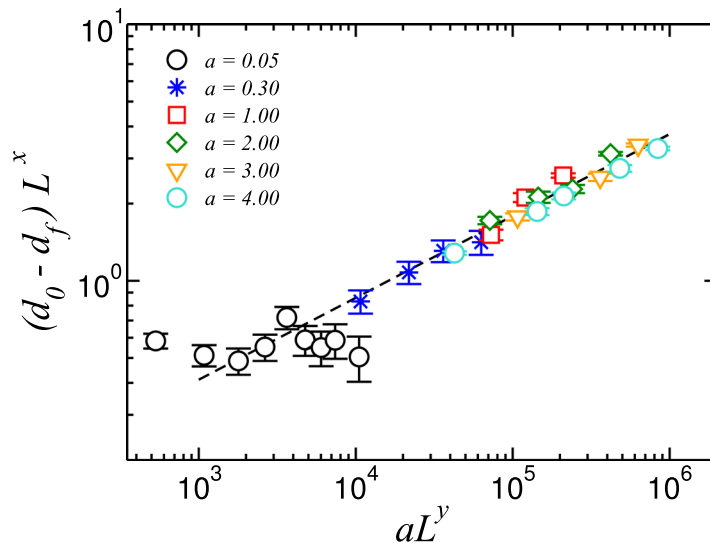


Figure 4. Scaling function for different parameters a and sizes L . The dashed line is a guide to the eye of slope $-x/y$.

Previous measurements of the fractal dimension of a watershed surface in three dimensions yielded a fractal dimension of 2.487 ± 0.003^{24} . One might naively identify the hydrological watershed as the cut between this three dimensional watershed with the surface of the landscape. Therefore, we could expect the hydrological watershed to have a fractal dimension of $2.487 - 1 = 1.487$. In what follows, we investigate the possibility that it might be possible that our numerical extrapolation $d_f = 1.31 \pm 0.02$ is only part of a crossover, with the hydrological watershed asymptotically having fractal dimension $d_f = 1.487$. For this purpose, we analyzed the finite size scaling behavior of the watershed. The ansatz for the scaling function is given by,

$$d_0 - d_f = L^{-x} F(aL^y), \quad (2)$$

where d_0 denotes the fractal dimension for $a = 0$ and $L \rightarrow \infty$, and x, y are scaling exponents. For our analysis, we chose to evaluate the scaling law for both $d_0 = 1.31$ and $d_0 = 1.487$. The scaling exponent x can be obtained using the relation, $d_0 - d_f \propto L^{-x}$, when setting $a = 0$. Assuming the same relation for $a = 0.05$, we get a first estimate for x . Then, plotting Eq. 2 as shown in Fig. 4, we obtain final values for x and y through the best data collapse for different a and L with the constraint that the slope in a log-log plot be $-x/y$. By choosing $d_0 = 1.487$, such a data collapse only becomes possible for very unlikely exponents, namely x being either 0.05 or y being 20. Setting $d_0 = 1.31$, yields $x = 0.56 \pm 0.05$ and $y = 1.75$, with a convincing data collapse (see Fig. 4). In this way, no realistic scaling function can be found for $d_0 = 1.487$, whereas for $d_0 = 1.31$ we observe data collapse for a reasonable choice of x and y . This suggests that we are not facing a crossover to the fractal dimension $d_f = 1.487$, but we have discovered, in fact, a new universality class for the hydrological watershed.

Discussion

The topological watershed which is directly obtained from the discrete elevation map has been studied extensively in the past^{21–24,32}. We found that the penetration of water into the soil not only modifies the topological watershed, but also changes its continuity, and even its fractal dimension. The value of the fractal dimension of the topological watershed in a two-dimensional model is known to be 1.2168 ± 0.0005^{24} . Our measurements for the fractal dimension show that the fractal dimension of a hydrological watershed is $d = 1.31 \pm 0.02$. Comparing this to the fractal dimension of a watershed surface in three dimensions and its fractal dimension of 2.487 ± 0.003^{24} , we first expected to obtain a fractal dimension of 1.487. We ruled out the possibility of our data being part of a crossover with a scaling analysis, which showed convincing data collapse for $d_f = 1.31 \pm 0.02$, but not for 1.487 ± 0.003 . We can therefore assert that the hydrological watershed belongs to a new universality class.

We obtained the measured fractal dimensions for a model of randomized linear permeability in uncorrelated soil. Our permeability model could very well be substituted with another soil generation method that allows for variations over the penetration depth of the water and which would be equally justifiable. Furthermore, a new soil generation method could account for spatial correlations that are occurring in real soils, which are described by a Hurst exponent $H^{23,33}$. It is relatively easy to extend our algorithm to a different soil generation method as it does not affect our watershed calculation method and measurement methodology.

References

- Horton, R. E. Erosional development of streams and their drainage basins; hydrophysical approach to quantitative morphology. *Geological society of America bulletin* **56**, 275–370 (1945).
- Strahler, A. N. Quantitative analysis of watershed geomorphology. *Transactions American Geophysical Union* **38**, 913–920 (1957).
- Band, L. E. Topographic partition of watersheds with digital elevation models. *Water resources research* **22**, 15–24 (1986).
- Porto, M., Bunde, A., Havlin, S. & Roman, H. E. Structural and dynamical properties of the percolation backbone in two and three dimensions. *Physical Review E* **56**, 1667–1675 (1997).
- Brooks, K. N., Ffolliott, P. F. & Magner, J. A. *Hydrology and the Management of Watersheds*. 4 edn (John Wiley & Sons, 2013).

6. Vörösmarty, C. J., Federer, C. A. & Schloss, A. L. Potential evaporation functions compared on us watersheds: Possible implications for global-scale water balance and terrestrial ecosystem modeling. *Journal of Hydrology* **207**, 147–169 (1998).
7. Knecht, C. L., Trump, W., ben Avraham, D. & Ziff, R. M. Retention capacity of random surfaces. *Physical review letters* **108**, 045703 (2012).
8. United Nations. Reports of international arbitral awards. http://legal.un.org/riaa/cases/vol_IX/37-49.pdf. Accessed: 2017-08-25 (1902).
9. Eidgenössisches Departement für auswärtige Angelegenheiten. Verlauf der grenze zwischen schweiz und italien. (2009). <https://www.admin.ch/gov/de/start/dokumentation/medienmitteilungen.msg-id-28489.html>. Accessed: 2017-08-25.
10. Saberi, A. A. Recent advances in percolation theory and its applications. *Physics Reports* **578**, 1–32 (2015).
11. Araújo, N. A. M., Grassberger, P., Kahng, B., Schrenk, K. J. & Ziff, R. M. Recent advances and open challenges in percolation. *The European Physical Journal Special Topics* **223**, 2307–2321 (2014).
12. Grau, V., Mewes, A. U. J., Alcaniz, M., Kikinis, R. & Warfield, S. K. Improved watershed transform for medical image segmentation using prior information. *IEEE Transactions on Medical Imaging* **23**, 447–458 (2004).
13. Ng, H. P., Ong, S. H., Foong, K. W. C., Goh, P. S. & Nowinski, W. L. Medical image segmentation using k-means clustering and improved watershed algorithm. In *Image Analysis and Interpretation, 2006 IEEE Southwest Symposium on*, 61–65 (IEEE, 2006).
14. Beucher, S. & Meyer, F. The morphological approach to segmentation: the watershed transformation. In *Mathematical Morphology in Image Processing* (Dougherty, E. R. (ed.)) chap. 12, 433–480 (Marcel Dekker, Inc., 1993).
15. Cousty, J., Bertrand, G., Najman, L. & Couprie, M. Watershed cuts: Thinnings, shortest path forests, and topological watersheds. *IEEE Transactions on Pattern Analysis and Machine Intelligence* **32**, 925–939 (2010).
16. Breyer, S. P. & Snow, R. S. Drainage basin perimeters: a fractal significance. *Geomorphology* **5**, 143–157 (1992).
17. Schrenk, K. J., Araújo, N. A. M., Andrade, J. S. & Herrmann, H. J. Fracturing ranked surfaces. *Scientific Reports* **2**, 348 (2012).
18. Braun, C., Dake, J. M., Krill, C. E. & Birringer, R. Abnormal grain growth mediated by fractal boundary migration at the nanoscale. *Scientific reports* **8**, 1592 (2018).
19. Cieplak, M., Maritan, A. & Banavar, J. R. Optimal paths and domain walls in the strong disorder limit. *Physical review letters* **72**, 2320 (1994).
20. Daryaei, E. & Rouhani, S. Loop-erased random walk on a percolation cluster: Crossover from euclidean to fractal geometry. *Physical Review E* **89**, 062101 (2014).
21. Couprie, M., Bertrand, G. *et al.* Topological grayscale watershed transformation. In *SPIE Vision Geometry V Proceedings*, vol. 3168, 136–146 (1997).
22. Fehr, E. *et al.* New efficient methods for calculating watersheds. *Journal of Statistical Mechanics: Theory and Experiment* **2009**, P09007 (2009).
23. Fehr, E., Kadau, D., Araújo, N. A. M., Andrade, J. S. & Herrmann, H. J. Scaling relations for watersheds. *Physical Review E* **84**, 036116 (2011).
24. Fehr, E. *et al.* Corrections to scaling for watersheds, optimal path cracks, and bridge lines. *Physical Review E* **86**, 011117 (2012).
25. Schrenk, K. J., Araújo, N. A. M. & Herrmann, H. J. How to share underground reservoirs. *Scientific reports* **751** (2012).
26. Andrade, J. S., Oliveira, E. A., Moreira, A. A. & Herrmann, H. J. Fracturing the optimal paths. *Physical Review Letters* **103**, 225503 (2009).
27. Porto, M., Havlin, S., Schwarzer, S. & Bunde, A. Optimal path in strong disorder and shortest path in invasion percolation with trapping. *Physical Review Letters* **79**, 4060–4062 (1997).
28. Daryaei, E., Araújo, N. A. M., Schrenk, K. J., Rouhani, S. & Herrmann, H. J. Watersheds are schramm-loewner evolution curves. *Physical Review Letters* **109**, 218701 (2012).
29. Wilkinson, D. & Willemsen, J. F. Invasion percolation: a new form of percolation theory. *Journal of Physics A: Mathematical and General* **16**, 3365 (1983).
30. Tricot, C., Quiniou, J. F., Wehbi, D., Roques-Carmes, C. & Dubuc, B. Evaluation de la dimension fractale d'un graphe. *Revue de Physique Appliquée* **23**, 111–124 (1988).
31. Park, S. K. & Miller, K. W. Random number generators: good ones are hard to find. *Communications of the ACM* **31**, 1192–1201 (1988).
32. Araújo, N. A. M., Schrenk, K. J., Herrmann, H. J. & Andrade, J. S. Watersheds in disordered media. *Frontiers in Physics* **3**, 5 (2015).
33. Mandelbrot, B. B. & Wallis, J. R. Noah, joseph, and operational hydrology. *Water resources research* **4**, 909–918 (1968).

Acknowledgements

We acknowledge financial support from the ERC Advanced grant number FP7-319968 FlowCCS of the European Research Council. We also acknowledge the agencies CNPq, CAPES, and FUNCAP, and the National Institute of Science and Technology for Complex Systems in Brazil for financial support.

Author Contributions

B.B., J.A. and H.H. designed research and wrote the paper. B.B. programmed the simulation and analyzed the data.

Additional Information

Competing Interests: The authors declare no competing interests.

Publisher's note: Springer Nature remains neutral with regard to jurisdictional claims in published maps and institutional affiliations.



Open Access This article is licensed under a Creative Commons Attribution 4.0 International License, which permits use, sharing, adaptation, distribution and reproduction in any medium or format, as long as you give appropriate credit to the original author(s) and the source, provide a link to the Creative Commons license, and indicate if changes were made. The images or other third party material in this article are included in the article's Creative Commons license, unless indicated otherwise in a credit line to the material. If material is not included in the article's Creative Commons license and your intended use is not permitted by statutory regulation or exceeds the permitted use, you will need to obtain permission directly from the copyright holder. To view a copy of this license, visit <http://creativecommons.org/licenses/by/4.0/>.

© The Author(s) 2018